J Physiol Sci (2014) 64:141–150
DOI 10.1007/s12576-013-0303-6

ORIGINAL PAPER

Electrostatic charge at position 552 affects the activation and permeation of FMRFamide-gated Na^+ channels

Yu Kodani · Yasuo Furukawa

Received: 30 October 2013 / Accepted: 27 December 2013 / Published online: 12 January 2014

Abstract The FMRFamide-gated Na^+ channel (FaNaC) is a unique peptide-gated sodium channel and a member of the epithelial sodium channel/degenerin family. Previous studies have shown that an aspartate residue (Asp^{552}) in the second transmembrane domain is involved in activation of the FaNaC. To examine the significance of a negative charge at position 552, we used a cysteine-modification method. Macroscopic currents of a cysteine mutant (D552C) were potentiated or inhibited by use of positively or negatively charged sulfhydryl reagents ([2-(trimethylammonium)ethyl]methanethiosulfonate bromide, MTSET, and sodium (2-sulfonatoethyl)methanethiosulfonate, MTSES, respectively). Dose–response analysis showed that treatment with MTSET increased the potency of the FMRFamide in the FaNaC whereas treatment with MTSES reduced the maximum response. Negative charge at position 552 was necessary for the characteristic inward rectification of the FaNaC. These results suggest that negative electric charge at position 552 is important to the activation and permeation properties of the FaNaC.

Keywords ENaC · ASIC · FaNaC · Cysteine modification · Sulfhydryl reagent · Rectification

Y. Kodani · Y. Furukawa (✉)
Laboratory of Neurobiology, Faculty of Integrated Arts and Sciences, Hiroshima University, Kagamiyama 1-7-1, Higashi-Hiroshima 739-8521, Japan
e-mail: yasfuru@hiroshima-u.ac.jp

Present Address:
Y. Kodani
Department of Physiology, Fujita Health University School of Medicine, Toyoake, Aichi 470-1192, Japan

Introduction

The FMRFamide-gated Na^+ channel (FaNaC) is a ligand-gated sodium channel that is activated by a neuropeptide, FMRFamide. Although FaNaCs have been cloned from mollusks only, related peptide-gated channels have been cloned from an evolutionarily more primitive animal, hydra [1], implying more widespread distribution of these related peptide-gated channels in the animal kingdom. Structurally, the FaNaC is a member of the epithelial sodium channel/degenerin (ENaC/DEG) family. Among the channels in this family, the acid-sensing ion channel (ASIC) activated by H^+ binding is most closely related to the FaNaC ($\sim$50 % homologous in amino acid sequences). Besides the overall structural similarity, some ASICs are known to be modulated by FMRFamide and related peptides [2], suggesting that ASICs have peptide-binding domains. Recent analysis of the ASIC3 has also shown it can be activated by small molecular agonists different from H^+ [3]. The mechanisms of the binding–gating conformational changes of the FaNaC and the ASIC may therefore be similar or related.

Crystal structures of chicken ASIC1 unequivocally show the channel is trimeric in structure [4, 5], which suggests that other members of the ENaC/DEG family also form trimeric channels. The subunits in the ENaC/DEG family have common membrane topology: i.e., two transmembrane domains (TM1 and TM2) are connected by a large extracellular domain. According to the crystal structure, the external domain is divided into subdomains, called the "thumb", "finger", "knuckle", "β-ball", and "palm" domains [5]. The junction between the extracellular domain and the membrane domain is called the "wrist", in which there are three fenestrations which open to the external mouth of the pore [5]. Many functional regions, including

the binding sites for H^+, are located in the extracellular domain, and the wrist region links the ligand-binding and opening conformational change of the transmembrane domain. Even before crystallographic studies, mutagenic studies of the ENaC/DEG family showed that highly conserved residues in the TM2 domain are involved in Na^+ selectivity and amiloride block, characteristics of ENaC/DEG family channels [6]. The results were consistent with the crystal structure of chicken ASIC1, in which the TM2 domain of each subunit surrounds the central axis of the transmembrane domain, that is, the channel pore [4, 5].

Several studies of the ENaC/DEG family also suggest that the N-termini of the transmembrane domains and the wrist region are involved in the conformational change during channel gating. Degenerins in *C. elegans* are ENaC/DEG family channels, and a mutation at a specific site of the N-terminus of the TM2 domain in degenerins (**d**-position) induces neurodegeneration [7, 8]. Substitution of an endogenous small-amino-acid residue at the **d**-position with a bulky amino acid makes the ENaC/DEG family channels constitutively active [9, 10, 11]. Analysis of some ENaC/DEG family channels by the substituted cysteine accessibility method (SCAM) showed that the **d**-position is exposed to the aqueous environment only when the channels are in the open states [10, 12], suggesting that a conformational change of the N-terminal region of the TM2 domain is necessary for channel opening. A recent study using voltage clamp fluorimetry and the SCAM also suggested that the region immediately preceding the TM2 domain undergoes conformational rearrangements during proton-dependent gating of the ASIC1 [13]. More specifically, the interaction between Tyr^{72} in a loop of the external domain and Trp^{288} in the N-terminus of the TM1 domain is essential for the link between H^+-binding and channel gating of the ASIC1 [14].

Among the FaNaCs so far cloned, two conserved acidic residues (Asp^{552} and Asp^{556} in the FaNaC of *Aplysia kurodai*, known as the AkFaNaC) are observed in the N-terminus of the TM2 domain [15], and are close to the **d**-position of the FaNaC (Ala^{555} in the AkFaNaC). An aspartate residue which corresponds to Asp^{556} is also conserved in the ASIC, and the aspartate has been shown to be involved in Ca^{2+} blocking of the ASIC [16]. In some ENaC/DEG family channels including the ENaC-α [17], the HyNaC [1], and the ASIC3 [18], the positions corresponding to Asp^{552} are also occupied by charged or ionizable amino acids, implying that electrostatic charge at this position may have a common functional effect in this channel family. We have previously shown that several mutations of Asp^{552} in the AkFaNaC affect the macroscopic activation, desensitization, and potency of FMRFamide [19]. As might be imagined, negative electric charge at position 552 seemed to be important, because the lysine-substituted mutant (D552K) was activated much more slowly than the wild-type channel, and its EC_{50} for FMRFamide was shifted to lower concentration. The importance of electrostatic charge was, however, partly obscured by the fact that replacing Asp^{552} with glutamate clearly reduced the potency of FMRFamide to activate the channel.

To better understand the functional contribution of position 552, in this study we focused on the effects of electrostatic charge at position 552. To determine the effects of electrostatic charge at this position, we used the cysteine mutant of the AkFaNaC (D552C) and examined macroscopic currents expressed in *Xenopus* oocytes before and after modification of the thiol in Cys^{552} by cationic or anionic methanethiosulfonate reagent. Our results showed that electrostatic charge at position 552 of the AkFaNaC is an important determinant of the activation and permeation properties of the FaNaC.

Materials and methods

Homology modeling

Structural models of the homo-trimeric *Aplysia kurodai* FaNaC (AkFaNaC) and its mutants were made by use of Modeller ver 9 [20]. As template we used a homo-trimeric structure of the desensitized chicken ASIC1 (Protein Data Bank, 3hgc.pdb, [4]) obtained from the protein interfaces, surfaces and assemblies service, PISA, at the European Bioinformatics Institute (http://www.ebi.ac.uk/msd-srv/prot_int/pistart.html, [21]). Among 50 models made by Modeller, we selected the model with the least molecular probability density function as an initial model. We next used FoldX (http://foldx.crg.es/, [22, 23]) or SCWRL4 (http://dunbrack.fccc.edu/scwrl4/, [24]) to refine the orientations of side-chains in the model. To locate the inner cavities of the modeled structure, we used ALLCHANNELEXC (http://3vee.molmovdb.org/) which detects inner cavities or channels connected to external solvent in a protein structure and makes MRC format files of detected cavities and channels [25]. CHIMERA (http://www.cgl.ucsf.edu/chimera/, [26]) was used to visualize the MRC files and to make structural figures.

Oocyte expression for electrophysiological recording

The wild-type AkFaNaC (WT) and its D552 mutants (D552C, D552E, D552N, D552K) were expressed in *Xenopus laevis* oocytes as described elsewhere [19]. Briefly, stage V–VI oocytes were injected with 1–10 ng cRNA encoding AkFaNaC or D552 mutants then incubated at 18 °C in ND96 (in mM: NaCl 96, KCl 2, $CaCl_2$ 1.8, $MgCl_2$ 1, HEPES 5, pH 7.5). We routinely injected cRNA

into the animal hemisphere of oocytes. After incubation for 2–5 days the oocytes were used for electrophysiological recording.

Electrophysiological recording

Whole-cell membrane currents in oocytes were measured by use of the two-electrode voltage clamp technique with the OC-725C (Warner Instruments, Hamden, CT, USA), essentially as described elsewhere [15, 19]. An oocyte was placed in a recording chamber (~100 μl) which was continuously perfused with ND96 (~2 ml/min). The bath probes of the OC-725C were connected to the chamber via 2 % agarose/1 M KCl bridges which were placed close to the oocyte. The holding potential was −50 mV throughout the study. We used agarose-cushioned microelectrodes [27] for both potential measurement and current injection. The tips of the electrodes were filled with 2 % agarose dissolved in 1.5 M KCl, and back-filled with 1.5 M KCl. The resistances of the electrodes were 0.5–3 MΩ. Use of agarose-cushioned electrodes seems to reduce rundown of the FaNaC currents, probably by preventing leakage of KCl into the cytosol. FMRFamide (Peptide Institute, Osaka, Japan) was applied by bath perfusion, as described elsewhere. All experiments were performed at room temperature (20–25 °C).

Steady-state membrane currents were measured by use of a slow ramp command from −100 to +80 mV at ~94 mV/s, as described elsewhere [15]. The ramp commands were applied before FMRFamide application and at the peak of the FMRFamide-gated current. To achieve a steady-state current-voltage (*I–V*) relationship, the membrane currents in response to the ramp command obtained before the FMRFamide application were subtracted from the currents obtained in the presence of FMRFamide.

Methanethiosulfonate (MTS) reagents

To alter the electric charge at position 552, we used a cysteine modification of D552C with [2-(trimethylammonium)ethyl]methanethiosulfonate bromide (MTSET) and sodium (2-sulfonatoethyl)methanethiosulfonate (MTSES) (Toronto Research Chemicals, Ontario, Canada). MTSET and MTSES have positively and negatively charged groups, respectively, and are similar in size [28]. Both reagents are frequently used for studies of the substituted-cysteine accessibility of ion channels [28].

Stock solutions of MTSET (0.1 M) and MTSES (0.5 M) were prepared in distilled water immediately before the experiments. The solutions were kept on ice and diluted appropriately with ND96 within 3 min before application. Usually, the external solution was replaced with 1 mM MTSET or 10 mM MTSES-containing solution, and oocytes were kept in the solution for 2 min. After the treatment, oocytes were washed by perfusion with ND96. Repeated treatment with MTS reagents or longer application did not change the results in these experiments.

We also examined the effect of a reducing reagent, dithiothreitol (DTT). Stock solution (1 M) of DTT (Nakarai Tesque, Kyoto, Japan) was prepared immediately before the experiments and diluted appropriately with ND96. We used 20–50 mM DTT in these experiments because lower concentrations were not effective. Practical concentration of DTT depends on accessibility of the DTT and similar high concentrations of DTT have been used in other studies [10, 29]. Oocytes were treated with DTT for 1 min and then washed. Treatment with 50 mM DTT had essentially no effect on FMRFamide-gated currents of WT examined 10–20 min after the treatment (data not shown).

Fluorescence labeling of Cys^{552}

To visualize the stability of the disulfide bond at position 552 of the AkFaNaC we treated oocytes expressing the D552C with a fluorescent thiol-reactive reagent, BODIPY TMR C_5-thiosulfate (Invitrogen, Carlsbad, CA, USA). To check background fluorescence, oocytes injected with distilled water or cRNA of WT were also prepared.

The oocytes were incubated in ND96 containing 100 μM BODIPY TMR C_5-thiosulfate for 2 min at room temperature with gentle agitation. The oocytes were then quickly washed three times with ND96, and were observed by use of a BZ-9000 (Keyence, Osaka, Japan) inverted fluorescence microscope. An oocyte was carefully placed in a well of a 24-well plate filled with ND96 to enable observation of the border between the animal and vegetal hemispheres. The oocyte was viewed with a 4× objective, and fluorescence images (1360 × 1024 pixels) were acquired every minute by use of the time-lapse imaging tool of the BZ-9000. Acquisition of the fluorescence images was started 3 min after labeling and continued for 30 min.

To quantify the intensity of fluorescence, we first selected a rectangular region including the animal hemisphere, and the brightness of the same region in each time-lapse image was calculated by use of EBImage [30], an image processing toolbox for an open-source statistical package, R (http://www.r-project.org/).

Data analysis

Digitized data were analyzed by use of Clampfit Ver. 6 (Axon Instruments), Origin Ver. 6 (Originlab, Northampton, MA, USA), or R. Grouped results were expressed as means ± SD. Statistical significance was assessed by use of the one sample *t*-test, the paired *t*-test, or the Wilcoxon rank sum test ($p < 0.05$ was considered to be significant).

The dose–response relationship for FMRFamide was obtained by measuring peak currents in response to different concentrations of FMRFamide. These were then fitted to a Hill equation:

$$I = I_{max}[A]^n/(EC_{50}^n + [A]^n) \quad (1)$$

where I is the amplitude of the current in response to a given concentration of FMRFamide, I_{max} is the maximum current estimated by fitting, [A] is the concentration of FMRFamide, EC_{50} is the concentration of FMRFamide that evokes half maximum response, and n is the Hill coefficient. The dose–response relationships before and after MTS treatment of each oocyte were then normalized to the estimated I_{max} before treatment.

The steady-state *I–V* relationship for the AkFaNaC shows clear inward rectification with small outward currents [15]. To qualify the curvature of *I–V* curve at more negative potentials than the reversal potential, we quantified the FMRFamide-gated currents by use of an equation of the form:

$$RI(V) = I_{ramp}(V) - I_{linear}(V) \quad (2)$$

where RI is a rectification index which is a function of the membrane potential (V), $I_{ramp}(V)$ is a steady-state *I–V* relationship obtained by the ramp pulse method described above, and $I_{linear}(V)$ is an arbitrary linear *I–V* relationship which passes the reversal potential of I_{ramp} and $I_{ramp}(-100)$. Both currents were normalized to $I_{ramp}(-100)$ before calculation of RI. Between the reversal potential and –100 mV, RI is 0 if the *I–V* relationship for the FMRFamide-gated currents is completely linear but has either a positive or negative value depending on the rectification of the steady-state *I–V* relationship.

Results

Fluorescence labeling of Cys^{552} by BODIPY TMR C_5-thiosulfate

We constructed 3D models of the homo-trimeric AkFaNaC on the basis of the crystal structure of the chicken ASIC1 [4, 5]. In the modeled structure of the AkFaNaC (Fig. 1a), several inner cavities were detected in the large extracellular domain as shown for the cASIC1 [4]. Among the cavities detected, that situated in the wrist region is of primary interest in this study (Fig. 1b). This cavity comprises the external vestibule of the channel pore and is connected to external solution via three fenestrations [4]. Asp^{552} of each subunit is near each fenestration, and located on the floor of this cavity (Fig. 1b).

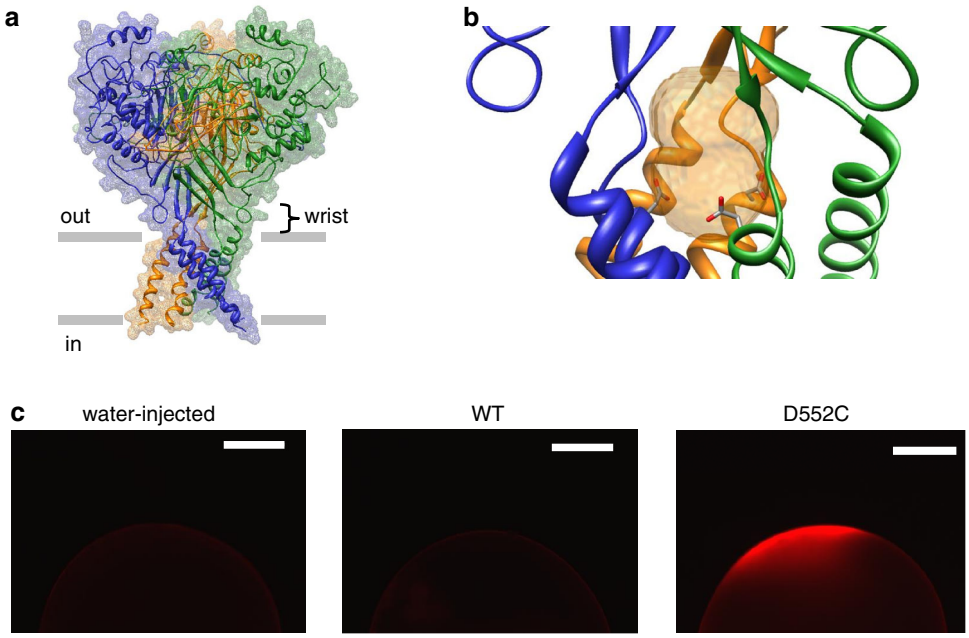

Fig. 1 Position of Asp^{552} in a 3D model of the FMRFamide-gated Na^+ channel, and fluorescence labeling of D552C with BODIPY TMR C_5-thiosulfate. **a** 3D model of the FMRFamide-gated Na^+ channel. The model was made by use of Modeller, and the orientations of the side-chains were refined by use of SCWRL4. **b** Close up view of the wrist region of the channel. The inner cavity of the external vestibule, shown by *transparent yellow*, in the wrist region was detected by use of ALLCHANNELEXC, with probe radii of 10 Å for "shell volume" and 4 Å for "solvent-excluded volume" [25]. Side-chains of the three Asp^{552}s are shown by use of stick models. **c** Fluorescence of water-injected, WT-expressing, or D552C-expressing oocyte after treatment with 100 μM BODIPY TMR C_5-thiosulfate for 2 min. The images show the fluorescence of the animal hemisphere of the oocytes 3 min after treatment. *Scale bars* indicate 300 μm

As described in the "Introduction", previously obtained physiological data suggest the side-chain at position 552 is exposed to the permeation pathway of the channel. If this is so, an introduced cysteine residue at position 552 (D552C) would be modified by methanethiosulfonic acid reagents and modification of the D552C may affect the permeation or gating property of the AkFaNaC. To visualize covalent modification of Cys^{552} we used BODIPY TMR C_5-thiosulfate, a fluorescent SH-reactive reagent. Oocytes were first incubated in BODIPY TMR C_5-thiosulfate for 2 min, and the fluorescence was then monitored in ND96 (described in "Materials and methods"). Because the reagent is membrane-impermeable, only externally accessible cysteine residues are fluorescently labeled by the disulfide bridge.

There are 14 endogenous cysteines in the AkFaNaC, all of which are conserved among the ENaC/DEG family channels; these form seven disulfide bonds in the thumb, palm, and β-ball domains of the cASIC1 [5]. Indeed, only weak background fluorescence over the cell surface was observed for water-injected and WT-expressing oocytes after treatment with 100 μM BODIPY TMR C_5-thiosulfate (Fig. 1c). By contrast, we observed intense fluorescence on the cell surface of D552C-expressing oocytes (Fig. 1c), indicating that Cys^{552} residues of the D552C channels expressed on the membrane surface were successfully labeled. The labeling also revealed that surface expression of exogenous channels is not uniform but confined to the cell surface near the cRNA-injected site. Fluorescent intensity calculated from time lapse images (as described in "Materials and methods") was stable more than 30 min with a minimum decrement (data not shown).

Effects of MTS reagents on the current amplitude of D552C

We next examined the effects of MTS reagents on FMRFamide-gated currents. FMRFamide-gated currents were evoked by bath perfusion of FMRFamide as described in "Materials and methods". After confirming the stability of FMRFamide-gated currents, either positively charged (1 mM MTSET) or negatively charged (10 mM MTSES) MTS was applied for 2 min. The effects of MTS reagents on the FMRFamide-gated currents were examined 10 min after treatment. In WT, the FMRFamide-gated currents before and after MTS treatment were essentially the same (Fig. 2), indicating that externally applied MTSET or MTSES has no obvious effects on WT. In contrast, MTSET treatment increased the FMRFamide-gated currents of the D552C, and MTSES treatment reduced the currents (Fig. 2). In either case, the modification of the FMRFamide-gated currents was stable during the experiments (more than 30 min). We obtained similar results if we applied MTS reagents in the presence of FMRFamide (data not shown).

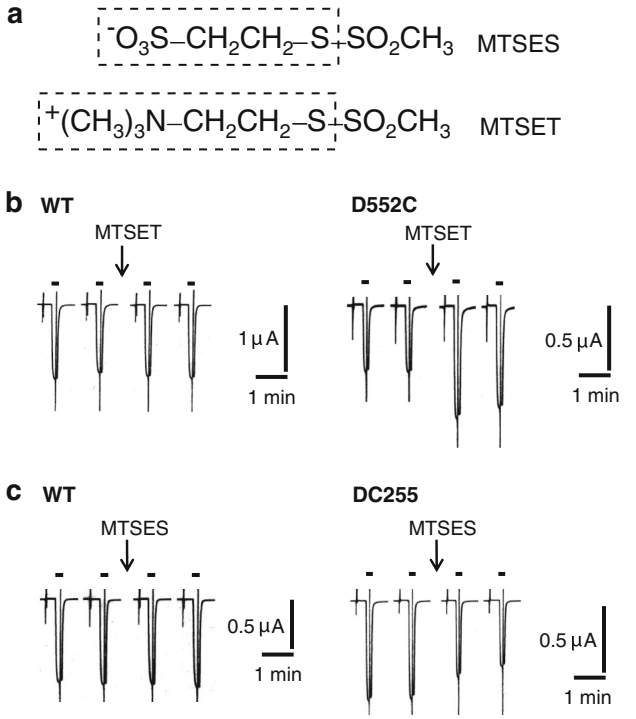

Fig. 2 Effects of MTS reagents on the current amplitude of WT and D552C. **a** Structures of MTSES and MTSET. A moiety enclosed in a *box* is appended to cysteine via a disulfide bond. **b** Representative recording showing effects of MTSET on WT and D552C. FMRFamide-gated currents were elicited by 1 μM FMRFamide for 20 s (*bars* indicate FMRFamide application). After measuring two consecutive FMRFamide-gated currents with an interval of 10 min, 1 mM MTSET was applied for 2 min (*arrow*). 10 min later, two consecutive FMRFamide-gated currents were evoked as before. **c** Representative recording showing effects of 10 mM MTSES on WT and D552C. FMRFamide-gated currents were evoked as described above (**b**). The steep vertical deflections are the currents in response to ramp commands, which are truncated for graphic reasons

Figure 3 shows a summary of modification of the FMRFamide-gated currents by MTS reagents and their reversal by the disulfide-reducing agent DTT. The mean amplitude of the D552C currents after MTSET treatment was 156.5 ± 27.6 % of the control; that after MTSES treatment was 68.8 ± 4.3 % of the control. Both of the effects are statistically significant ($p < 0.05$, Wilcoxon rank sum test). The effects of MTS reagents were almost completely abolished by DTT.

Effects of MTSET and MTSES on the FMRFamide dose–response relationship of the D552C

We next examined the dose–response relationships of the D552C before and after modification by use of MTS reagents (Fig. 4). As described previously, EC_{50} and the

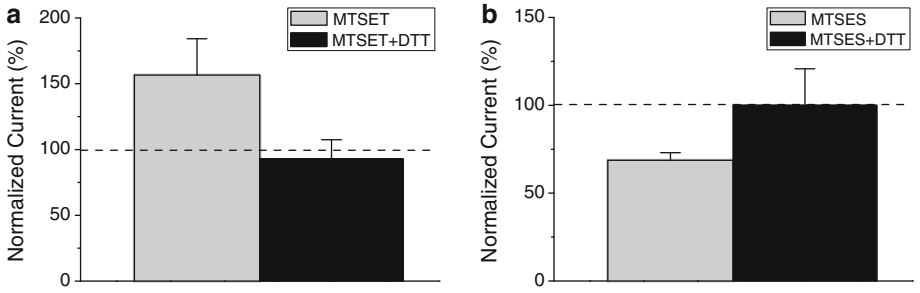

Fig. 3 Reversal of MTS modification by DTT. **a** Normalized current amplitude (mean ± SD) after treatment with MTSET (1 mM, 2 min, $n = 9$) or MTSET + DTT (2 min treatment with 1 mM MTSET was followed by 1 min treatment with 50 mM DTT, $n = 3$). The currents were normalized to control currents obtained just before the treatments. **b** Normalized current amplitude after treatment with MTSES (10 mM, 2 min, $n = 5$) or MTSES + DTT (2 min treatment with 10 mM MTSES was followed by 1 min treatment with 50 mM DTT, $n = 3$)

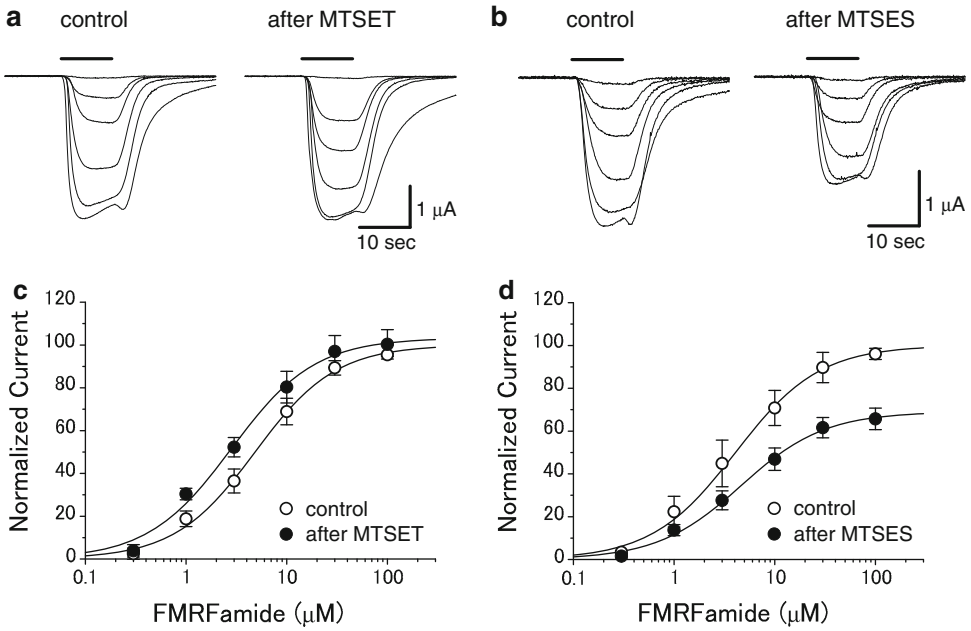

Fig. 4 FMRFamide dose–response relationships for the D552C before and after treatment with MTS reagents. **a** Representative FMRFamide-gated currents before and after treatment with 1 mM MTSET. FMRFamide was applied as indicated by a *bar*. FMRFamide concentration was 0.3, 1, 3, 10, 30, or 100 μM. **b** Representative FMRFamide-gated currents before and after treatment with 10 mM MTSES. FMRFamide was applied as described above (**a**). **c** Dose–response relationships before and after MTSET treatment ($n = 4$). *Smooth lines* are best fits to the Hill equation (Eq. 1, "Materials and methods"). EC_{50} values before and after the treatment were 4.85 ± 1.16 and 2.83 ± 0.17 μM, respectively. Hill coefficients before and after the treatment were 1.08 ± 0.01 and 1.05 ± 0.07, respectively. Maximum response became 103.3 ± 6.6 % of the control after the treatment. **d** Dose–response relationships before and after MTSES treatment ($n = 4$). EC_{50} values before and after the treatment were 4.08 ± 1.35 and 4.63 ± 1.39 μM, respectively. Hill coefficients before and after the treatment were 1.04 ± 0.13 and 1.04 ± 0.06, respectively. Maximum response became 69.0 ± 5.8 % of the control after the treatment

Hill coefficient of the D552C were similar to those of the WT [19]. Treatment with MTSET shifted the dose–response curve of the D552C to lower concentration (Fig. 4a, c). Fitting to the Hill equation revealed a slight but significant decrease of EC_{50} value (4.85 ± 1.16 vs 2.83 ± 0.17 μM, $p < 0.05$, paired *t*-test) without changing the Hill coefficient (1.08 ± 0.01 vs 1.05 ± 0.07, $p > 0.3$, paired *t*-test). The maximum response was not affected (103.3 ± 6.6 %, $p > 0.3$, one-sample *t*-test). Although the extent of the shift is modest, the fitted dose–response relationships show that an increase of the peak current of ~70 % is expected on addition of 1 μM FMRFamide after MTSET treatment. This is consistent with the result shown in Fig. 3a. By contrast, MTSES treatment (Fig. 4b, d) did not change EC_{50} (4.08 ± 1.35 vs 4.63 ± 1.39 μM, $p > 0.3$, paired *t*-test) or the Hill coefficient (1.04 ± 0.13

vs 1.04 ± 0.06, $p > 0.3$, paired *t*-test) but significantly reduced the maximum response (69.0 ± 5.8 %, $p < 0.005$, one-sample *t*-test). From the fitted dose–response relationships, a decrease of the peak current of ~40 % is expected on addition of 1 μM FMRFamide after MTSES treatment; this, again, is consistent with the result in Fig. 3b. These results suggest that electrostatic charge at position 552 is critical for activation of the AkFaNaC.

Electrostatic charge at position 552 is a critical determinant of current rectification in the AkFaNaC

The steady-state current-voltage (*I–V*) relationship for the wild-type AkFaNaC is clearly indicative of inward rectification [19]. Because previous mutagenic experiments [15] and these modeling results (Fig. 1) show that position 552 is in the external vestibule of the channel pore, electrostatic charge at this position may affect the permeation properties of the channel.

We therefore next examined whether the electrostatic charge at position 552 affects the steady-state *I–V* relationship of the AkFaNaC. Figure 5a shows the *I–V* relationships for the WT and D552 mutants obtained by use of slow voltage ramp commands from −100 to +80 mV. Although the reversal potentials of the D552 mutants were similar to that of the WT [19], the shapes of *I–V* relationships were clearly different (Fig. 5a). To compare the extent of rectification, we calculated RI values as described in "Materials and methods". RI values for the WT, D552E, D552C, D552N, and D552K between –80 and +40 mV are illustrated in Fig. 5c. The RI for the WT was a bell-shaped function of the membrane potential, and was concave downward, reflecting inward rectification of the WT. As might be expected, the RI of the D552E was similar to that

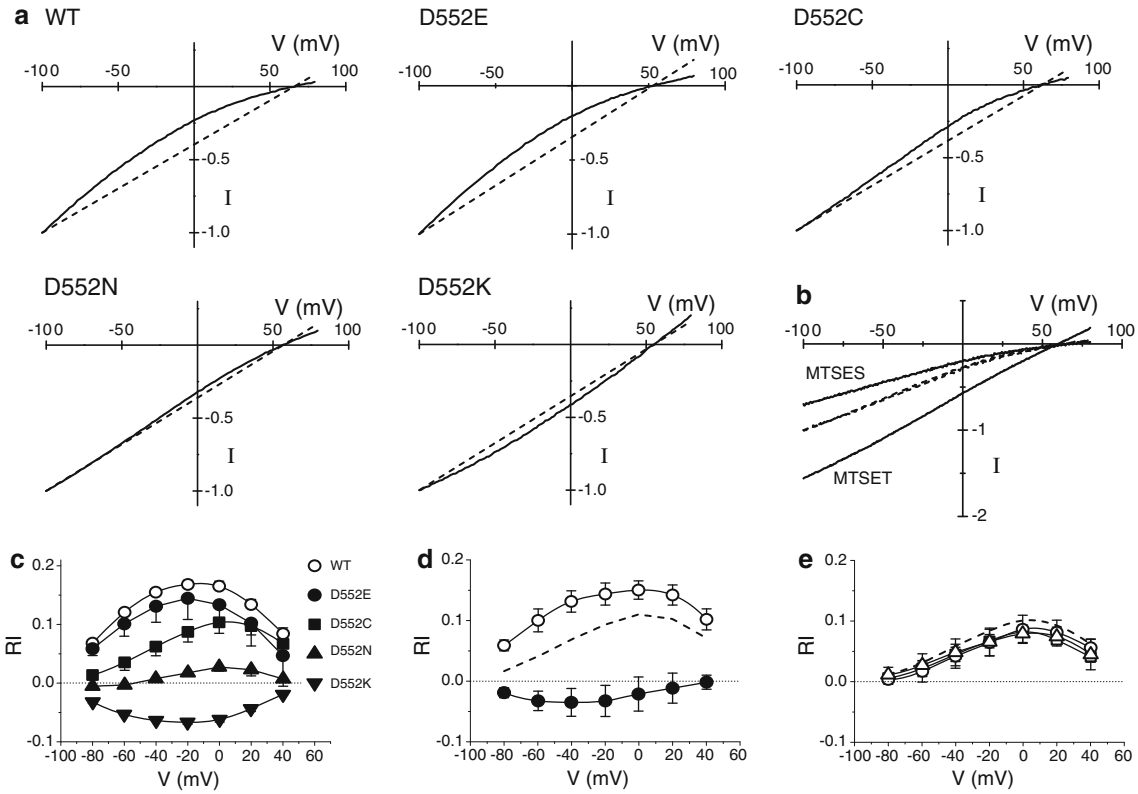

Fig. 5 Effects of charge alteration at position 552 on the *I–V* relationships of the AkFaNaC. **a** Steady-state *I–V* relationship of the WT, D552E, D552C, D552N, and D552K. In each figure, the *solid curve* shows a normalized steady state *I–V* relationship obtained as described in "Materials and methods". *The dashed line* is a straight line connecting the reversal potential and the current at −100 mV. **b** Steady-state *I–V* relationship for the MTSET-modified D552C or the MTSES-modified D552C. The concentrations of MTSET and MTSES were 1 and 10 mM, respectively. *I–V* relationships before MTS treatment are shown by *broken lines*. Currents were normalized to the current at −100 mV before MTS treatment. **c** Rectification index (RI) of the WT ($n = 6$), D552E ($n = 3$), D552C ($n = 25$), D552N ($n = 6$), and D552K ($n = 3$). The RI was calculated as described in "Materials and methods". **d** Modification by MTS reagents of the steady-state *I–V* relationship for the D552C. RI values obtained after treatment with 10 mM MTSES (*open circles*, $n = 4$) and 1 mM MTSET (*closed circles*, $n = 9$) are shown. *The dashed line* is the mean RI for the D552C before MTS treatment. **e** DTT reverses MTS reagent-induced modification of the *I–V* relationship for the D552C. RI values after treatment with 50 mM DTT (*squares*, $n = 4$), 1 mM MTSET followed by 50 mM DTT (*circles*, $n = 3$), and 10 mM MTSES followed by 50 mM DTT (*triangles*, $n = 3$) are shown. *The dashed line* is the mean RI for the D552C before MTS and/or DTT treatment

of the WT, showing clear inward rectification. The RI of the D552C was also concave downward but the amplitude was smaller, which was indicative of less inward rectification for the D552C. The RI of the D552N was close to zero, indicating that rectification for this mutant is very weak. In contrast, the RI for the D552K was concave upward, corresponding to outward rectification.

We next examined the effects of the MTS reagents on RI for the D552C. The *I–V* relationships were obtained 20–30 min after MTS treatment, as described above. The shape of *I–V* curve for the D552C but not for the WT changed after MTS treatment. For all of the voltage range examined, MTSET treatment increased the current of the D552C and MTSES treatment reduced the current (Fig. 5b). The RI of the MTS-treated D552C is shown in Fig. 5d. The RI became concave upward after treatment with MTSET (closed circles in Fig. 5d); this behavior is qualitatively similar to that of the D552K (compare Fig. 5c, d). By contrast, the RI of the D552C after MTSES treatment (open circles in Fig. 5d) was close to that of the WT, indicating that reduced inward rectification induced by the D552C mutation is restored by MTSES treatment. The effects of MTSET and MTSES were reversed by DTT treatment (Fig. 5e). Taken together, these results suggest that the negative charge of Asp^{552} is essential for inward rectification of the AkFaNaC.

Discussion

By using the cysteine modification technique with charged MTS reagents we studied the effects of charge alterations at position 552 of the AkFaNaC. This approach can enable direct comparison of current amplitudes before and after charge alteration. Our results indicate that the electrostatic moiety in the region of position 552 affects activation and permeation of the AkFaNaC.

Treatment with MTSET enhanced the current amplitude of FMRFamide-gated currents in the D552C whereas treatment with MTSES reduced the amplitude. Effects of the MTS reagents were stable and reversed by treatment with DTT, suggesting that the effects are because of covalent modification of the thiol of Cys^{552} by a cationic or anionic moiety. MTSET and MTSES are comparable in their size but have opposite electric charges [28], suggesting that their contrasting effects result from electrostatic effects on the side-chain attached to position 552.

We have previously shown that the EC_{50} of the D552C is similar to that of the WT [19]. Modification by MTSET reduced the EC_{50} of the D552C without affecting the maximum response. These results are qualitatively consistent with our previous finding that substitution of Asp^{552} by a positively charged amino acid (lysine; D552K) reduces the EC_{50} of the AkFaNaC [19]. The extent of the shift in the dose–response relationship was, however, clearly different for D552K and the MTSET-modified D552C: the EC_{50} for the D552K is a factor of approximately 20 less than that for the WT [19], whereas the EC_{50} for the MTSET-modified D552C was, at most, a factor of approximately 2 less than that of the D552C or the WT. Another notable difference between the D552K and the MTSET-modified D552C is their kinetics of activation. The D552K is activated sluggishly compared with the WT [19], whereas the activation kinetics of the MTSET-modified D552C were similar to those of the unmodified D552C or WT.

The difference between the D552K and the MTSET-modified D552C may be at least partly explained by the different size of their side-chains. Because the side-chain of the MTSET-modified cysteine is more bulky than that of lysine, their steric interactions with other parts of the channel and their electrostatic effects would not be the same. The importance of such steric properties, irrespective of electric charges at position 552 of the FaNaC, have already been reported [19].

In a previous study, the effect of negative charge at position 552 was difficult to understand because:

1 neutralization of the endogenous negative charge (Asp^{552}) by substituted asparagine (D552N) does not significantly alter EC_{50} and the Hill coefficient; and
2 substitution of Asp^{552} by glutamate (D552E) markedly increases the EC_{50} of the AkFaNaC [19].

In this study, MTSES treatment did not affect the EC_{50} value or the Hill coefficient of the D552C but significantly reduced the maximum response. In contrast, MTSET treatment reduced the EC_{50} slightly without affecting the maximum response. The qualitatively contrasting results for steady-state activation of the D552C after MTSET and MTSES treatment show rather clearly that, if the total volume of the side-chain is not very different, positive electric charge at position 552 favors channel opening.

Because position 552 is close to the **d**-position and to other positions whose side-chains are believed to move upon gating of the ENaC/DEG family of channels (discussed in the "Introduction"), the side-chain at position 552 may move more or less during channel gating. We have previously shown that physicochemical properties of the side-chain at position 552 of the AkFaNaC affect several properties of the channel but FMRFamide-dependent activation itself is not disturbed by large changes of side-chain size at this site [19]. For example, both the alanine-substituted (D552A) and tryptophan-substituted (D552W) mutants have similar EC_{50}. These results are counterintuitive if position 552 must move substantially during the conformation change which accompanies FMRFamide-dependent opening. We believe the side-chain of Asp^{552} of

the FaNaC is rather static and mostly exposed to the lumen of the external vestibule. This consideration is consistent with the results from our MTS-modification experiments at this position and with the static images of the 3D model made by homology modeling (Fig. 1). In agreement with this consideration, Tolino et al. [31] recently showed that a cysteine mutant of the mouse ASIC1a (G428C), which corresponds to the D552C, is modified by MTS reagent in both the resting and desensitized states. Moreover, a double mutant of mASIC1a, Y424C-G428C, expresses a functional acid-sensing channel in which Cys^{424} and Cys^{428} from different subunits are connected by disulfide bonds [31]. These results clearly show that restricted movement of the side-chain at position 428 does not hamper opening conformational change of the ASIC.

The wild-type AkFaNaC has clear inward rectification in *Xenopus* oocytes [15]. In this study we found that the charge alteration at position 552 has a critical effect on the current rectification of the AkFaNaC without noticeably affecting the reversal potential. The steady-state *I–V* relationship of the D552E was comparable with that of the WT, showing that inward rectification of the AkFaNaC is maintained in this mutant. However, the inward rectification was weakened in the D552C and was almost absent in the D552N. The inward rectification of the D552C was restored by treatment with MTSES, whereas the rectification became outward if D552C was treated with MTSET. The *I–V* relationship of the MTSET-modified D552C became close to that of the D552K. Taken together, these results suggest that the negative charge at position 552 is an important determinant of surface negativity in the external vestibule, and that the inward rectification of the AkFaNaC is at least partly due to the negative charge at position 552. Although the detailed mechanisms of the inward rectification of the AkFaNaC remain to be resolved, it is likely that Asp^{552} in the external vestibule interacts with permeant and impermeant cations entering through the fenestrations in the wrist region. Indeed, we have previously shown that the blocking action of external Ca^{2+} is much less for some D552 mutants, including the D552N and the D552K [19].

In conclusion, these and previous results from our laboratory show that the electric charge at position 552 is an important determinant of the channel gating and permeation of the FaNaC. As described in the "Introduction", the corresponding position in some other ENaC/DEG family channels is also occupied by a charged or ionizable amino acid. The position, therefore, may share some common functionality in the gating and/or permeation among the ENaC/DEG family channels.

Acknowledgments This work was partly supported by a Grant-In-Aid for Scientific Research to YF (nos 18570071, 20570071) from the Ministry of Education, Culture, Sports, Science, and Technology of Japan.

Conflict of interest The authors declare that they have no conflict of interest.

References

1. Golubovic A, Kuhn A, Williamson M, Kalbacher H, Holstein TW, Grimmelikhuijzen C.J.P, Gründer S (2007) A peptide-gated ion channel from the freshwater polyp *Hydra*. J Biol Chem 282:35098–35103
2. Lingueglia E, Deval E, Lazdunski M (2006) FMRFamide-gated sodium channel and ASIC channels: a new class of ionotropic receptors for FMRFamide and related peptides. Peptides 27:1138–1152
3. Yu Y, Chen Z, Li WG, Cao H, Feng EG, Yu F, Liu H, Jiang H, Xu TL (2010) A nonproton ligand sensor in the acid-sensing ion channel. Neuron 68:61–72
4. Gonzales EB, Kawate T, Gouaux E (2009) Pore architecture and ion sites in acid-sensing ion channels and P2X receptors. Nature 460:599–604
5. Jasti J, Furukawa H, Gonzales EB, Gouaux E (2007) Structure of acid-sensing ion channel 1 at 1.9 Å resolution and low pH. Nature 449:316–323
6. Kellenberger S, Schild L (2002) Epithelial sodium channel/degenerin family of ion channels: a variety of functions for a shared structure. Physiol Rev 82:735–767
7. Driscoll M, Chalfie M (1991) The *mec-4* gene is a member of a family of *Caenorhabditis elegans* genes that can mutate to induce neuronal degeneration. Nature 349:588–593
8. Huang M, Chalfie M (1994) Gene interactions affecting mechanosensory transduction in *Caenorhabditis elegans*. Nature 367:467–470
9. Brown AL, Fernandez-Illescas SM, Liao Z, Goodman MB (2007) Gain-of-function mutations in the MEC-4 DEG/ENaC sensory mechanotransduction channel alter gating and drug blockade. J Gen Physiol 129:161–173
10. Snyder PM, Bucher DB, Olson DR (2000) Gating induces a conformational change in the outer vestibule of ENaC. J Gen Physiol 116:781–790
11. Waldmann R, Champigny G, Voilley N, Lauritzen I, Lazdunski M (1996) The mammalian degenerin MDEG, an amiloride-sensitive cation channel activated by mutations causing neurodegeneration in *Caenorhabditis elegans*. J Biol Chem 271:10433–10436
12. Adams CM, Snyder PM, Price MP, Welsh MJ (1998) Protons activate brain Na^+ channel 1 by inducing a conformational change that exposes a residue associated with neurodegeneration. J Biol Chem 273:30204–30207
13. Passero CJ, Okumura S, Carattino MD (2009) Conformational changes associated with proton-dependent gating of ASIC1a. J Biol Chem 284:36473–36481
14. Li T, Yang Y, Canessa CM (2009) Interaction of the aromatics Tyr-72/Trp-288 in the interface of the extracellular and transmembrane domains is essential for proton gating of acid-sensing ion channels. J Biol Chem 284:4689–4694
15. Furukawa Y, Miyawaki Y, Abe G (2006) Molecular cloning and functional characterization of the *Aplysia* FMRFamide-gated Na^+ channel. Pflügers Arch 451:646–656
16. Paukert M, Babini E, Pusch M, Gründer S (2004) Identification of the Ca^{2+} blocking site of acid-sensing ion channel (ASIC) 1: implications for channel gating. J Gen Physiol 124:383–394
17. Canessa CM, Horisberger JD, Rossier BC (1993) Epithelial sodium channel related to proteins involved in neurodegeneration. Nature 361:467–470

18. Waldmann R, Bassilana F, de Weille J, Champigny G, Heurteaux C, Lazdunski M (1997) Molecular cloning of a non-inactivating proton-gated Na^+ channel specific for sensory neurons. J Biol Chem 272:20975–20978
19. Kodani Y, Furukawa Y (2010) Position 552 in a FMRFamide-gated Na^+ channel affects the gating properties and the potency of FMRFamide. Zool Sci 27:440–448
20. Šali A, Blundell TL (1993) Comparative protein modelling by satisfaction of spatial restraints. J Mol Biol 234:779–815
21. Krissinel E, Henrick K (2007) Inference of macromolecular assemblies from crystalline state. J Mol Biol 372:774–797
22. Guerois R, Nielsen JE, Serrano L (2002) Predicting changes in the stability of proteins and protein complexes: a study of more than 1000 mutations. J Mol Biol 320:369–387
23. Schymkowitz JWH, Rousseau F, Martins IC, Ferkinghoff-Borg J, Stricher F, Serrano L (2005) Prediction of water and metal binding sites and their affinities by using the Fold-X force field. PNAS 102:10147–10152
24. Krivov GG, Shapovalov MV, Dunbrack RL Jr (2009) Improved prediction of protein side-chain conformations with SCWRL4. Proteins 77:778–795
25. Voss NR, Gerstein M (2010) 3V: cavity, channel and cleft volume calculator and extractor. Nucl Acid Res 38:W555–W562
26. Pettersen EF, Goddard TD, Huang CC, Couch GS, Greenblatt DM, Meng EC, Ferrin TE (2004) UCSF Chimera—a visualization system for exploratory research and analysis. J Comput Chem 25:1605–1612
27. Schreibmayer W, Lester HA, Dascal N (1994) Voltage clamping of *Xenopus laevis* oocytes utilizing agarose-cushion electrodes. Pflügers Arch 426:453–458
28. Karlin A, Akabas MH (1998) Substituted-cystein accessibility method. Method Enzymol 293:123–145
29. Teichman S, Kanner BI (2007) Aspartate-444 is essential for productive substrate interactions in a neuronal glutamate transporter. J Gen Physiol 129:527–539
30. Pau G, Fuchs F, Sklyar O, Boutros M, Huber W (2010) EBImage—an R package for image processing with applications to cellular phenotypes. Bioinformatics 26:979–981
31. Tolino LA, Okumura S, Kashlan OB, Carattino MD (2011) Insights into the mechanism of pore opening of acid-sensing ion channel 1a. J Biol Chem 286:16297–16307